Polyoxometalate-Based Compounds for Photo- and Electrocatalytic Applications

Ning Li, Jiang Liu,* Bao-Xia Dong,* and Ya-Qian Lan*

P*hoto/electrocatalysis of water (H_2O) splitting and CO_2 reduction reactions is a promising strategy to alleviate the energy crisis and excessive CO_2 emissions. For the hydrogen evolution reaction (HER), oxygen evolution reaction (OER), and CO_2 reduction reaction (CO_2RR) involved, the development of effective photo/electrocatalysts is critical to reduce the activation energy and accelerate the sluggish dynamics. Polyoxometalate (POM)-based compounds with tunable compositions and diverse structures are emerging as unique photo/electrocatalysts for these reactions as they offer unparalleled advantages such as outstanding solution and redox stability, quasi-semiconductor behaviour, etc. This Minireview provides a basic introduction related to photo/electrocatalytic HER, OER and CO_2RR, followed by the classification of pristine POM-based compounds toward different catalytic reactions. Recent breakthroughs in engineering POM-based compounds as efficient photo/electrocatalysts are highlighted. Finally, the advantages, challenges, strategies and outlooks of POM-based compounds on improving photo/electrocatalytic performance are discussed.*

1. Introduction

In recent years, continuous and dramatic consumption of non-renewable fossil fuels (such as coal, oil, etc.) has induced a serious energy crisis, and a large amount of anthropogenic CO_2 discharged into the atmosphere has led to global climate changes such as greenhouse effect.[1] According to the reports of the International Energy Agency (IEA), global energy-related CO_2 emissions reached an all-time high of 33.0 Gt in 2019 and are predicted to increase up to 36–43 Gt by 2035. Under these circumstances, the best and most fundamental way to solve these threats is to find alternative renewable and clean energy sources and achieve effective conversion and utilization of CO_2.

Photo/electrocatalytic water splitting and CO_2 reduction reactions are believed to be the most promising pathways for efficient sustainable energy generation and conversion by using low-cost and renewable solar energy or electricity as driving force.[2] On the one hand, photo/electrocatalysis of water can generate eco-friendly hydrogen (H_2) and oxygen (O_2), and H_2 is an ideal energy carrier to replace traditional fossil fuels because of its clean combustion characteristics and high energy density. On the other hand, photo/electroreduction of CO_2 into value-added carbon-based products, including hydrocarbon fuels (such as CH_4, C_2H_4, C_2H_6) or chemicals (such as HCOOH, CH_3OH, CH_3COOH), represents an important and sustainable approach for natural carbon recycling. In these two clean energy conversion technologies, three types of redox reactions, hydrogen evolution reaction (HER), oxygen evolution reaction (OER, that is, water oxidation) and CO_2 reduction reaction (CO_2RR), are involved. In consideration of high reaction activation barriers, such reactions have to rely on the efficient photo/electrocatalysts to promote key proton-assisted multi-electron trans-

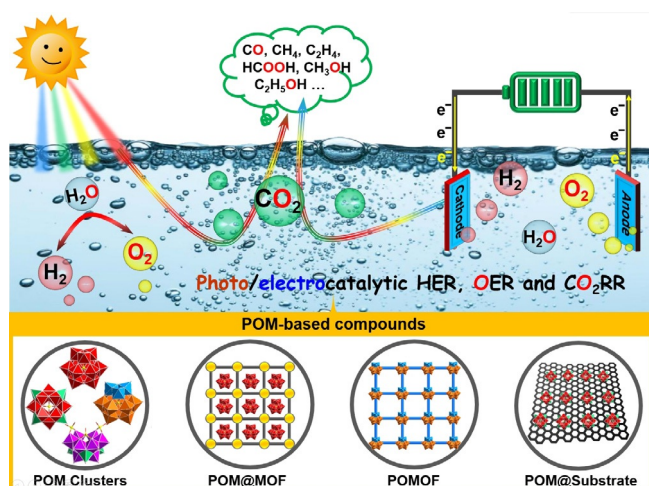fer processes for the formation of target oxidative and reductive products.

Polyoxometalates (POMs) are a large class of metal (e.g. V^V, Mo^V, Nb^V, Ta^V, Mo^{VI}, and W^{VI}) oxides that represent a tremendous range of crystalline inorganic clusters with an unmatched range of physical and chemical properties.[3] A large number of POM structures have been reported so far and their corresponding properties such as solubility, redox ability, acidity, thermal-/chemical stability can be adjusted by changing constituent elements, organic bridging components and structural dimensions (e.g. POM-based chains, layers and frameworks).[4] Moreover, many plenary POMs (include myriad d-electron-metal and/or f-electron-metal-substituted POMs) exhibit good pH, solvent, thermal and redox stability, thus they can be further used as building blocks for the design and assembly of covalence/coordination bond-integrated hybrid organic-inorganic frameworks. Most importantly, these POM-based compounds can usually display reversible multi-electron redox transformations while keeping stable structures, making them attractive for diverse photo/electrocatalytic applications. Up to now, many POM-based compounds involving POM clusters, POM@MOFs (POM molecule encapsulated into metal-organic frameworks), POMOFs (POM-based metal-organic frameworks) and POM@Substrates (POM molecule deposited onto conductive substrates) have been explored extensively in photo/electrocatalytic HER,[5] OER[6] and CO_2RR[7] (Scheme 1). Although they show some outstanding advantages and important progress in these reactions, there are still some serious problems that need to be further addressed. For example, under photo/electrocatalytic test conditions, the structural stability of the solid-state compound is still insufficient (they likely decomposed to generate other species on surfaces) and large single crystal sizes exhibit low catalytic activity. On the other hand, most of the reported POM-based compounds are insulating and have weak electronic conductivity, which greatly limits the improvement of photo/electrocatalytic performance. Currently, many POM-

[*] N. Li, Prof. B.-X. Dong
School of Chemistry and Chemical Engineering, Yangzhou University
Yangzhou 225002 (P. R. China)
E-mail: bxdong@yzu.edu.cn

Dr. J. Liu, Prof. Y.-Q. Lan
College of Chemistry and Materials Science, Nanjing Normal University
NanJing 210023 (China)
E-mail: liuj@njnu.edu.cn
yqlan@njnu.edu.cn

The ORCID identification number(s) for the author(s) of this article can be found under https://doi.org/10.1002/anie.202008054.

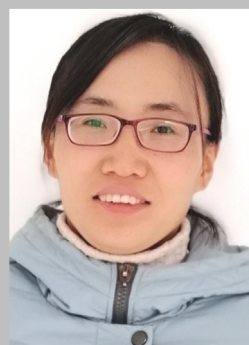**Scheme 1.** POM-based compounds for efficient photo/electrocatalytic applications including HER, OER and CO_2RR.

based photo/electrocatalytic studies are using amorphous systems, and important progress has been made for nanostructuring of POM-based compounds.[5i, 6o–q, 7g–h] Crystalline POM-based compounds are good candidates to serve as V, Mo, and W sources to produce the corresponding low-valence metal carbides, oxides, phosphides, and sulfides by pyrolysis at high temperature, which has been proven to display excellent HER, OER and CO_2RR performance. Furthermore, these POM-derived electrocatalysts after pyrolysis commonly show enhanced electronic conductivity and uniform distribution of active sites. However, the calcined electrocatalyst sometimes due to the complexed or unclear structural composition is always difficult to study the electrocatalytic reaction mechanism. In this Minireview, we mainly focus on the advantages,

recent advances and challenges of pristine POM-based compounds as photo/electrocatalysts applied for HER, OER and CO_2RR reactions. Finally, we outline the advantages and challenges of POM-based compounds as photo/electrocatalysts and propose some strategies and future perspectives that pull them to move forward.

2. POM-based compounds for photocatalysis

2.1. Hydrogen Production

Storable, clean, and renewable hydrogen has been treated as one kind of important substitute of fossil fuel, thus considerable attention is directed towards searching effective, low-cost and sustainable ways for the evolution of hydrogen energy. On this foundation, water splitting is believed to be a promising approach to produce renewable hydrogen and oxygen from water on a large scale and has attracted much attention in the past few decades (Figure 1). HER involving two electron transfer process is an essential half reaction of water splitting, and renewable solar/electrical power is often used as driving force (i.e. energy source) for this reaction. From thermodynamically, all the redox couples with a more reductive potential than the couple $E(H_2O/H_2)$ can reduce protons/H_2O into molecular H_2. However, this uphill reaction that has high Gibbs free energy requirement is often kinetically sluggish in the absence of a suitable photocatalyst. Thus, the development of the efficient semiconductor photocatalysts is fundamental and important to speed up the reaction dynamics. Typically, the efficient semiconductor photocatalyst materials for HER should have at least two basic features, a suitable optical band gap for collecting photons and a more negative bottom level of the conduction band than the redox
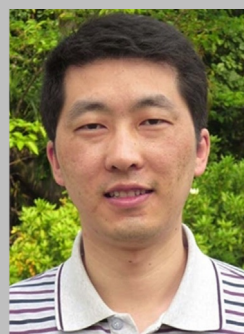
Ning Li received her master's degree (2013) under the supervision of Prof. Lifang Zhang at Shanxi Normal University. She is currently pursuing her Ph.D. study under the supervision of Prof. Baoxia Dong (Yangzhou University) and Prof. Ya-Qian Lan (Nanjing Normal University). Her research interest focuses on the synthesis and photo/electrocatalytic applications of new POMs, MOFs and titanium-oxo clusters.

Baoxia Dong is a Professor at Yangzhou University. She received her Ph.D. in Inorganic Chemistry from Northeast Normal University in 2007. She then worked at the National Institute of Advanced Industrial Science and Technology (AIST), and Hiroshima University, Japan, as Postdoctoral and Research Fellow (2007–2011). Her current research interests include the functional polyoxometalates and the development of new materials for electrochemical reduction of CO_2.

Jiang Liu received his Ph.D. degree (2016) under the supervision of Prof. Ming-Liang Tong at Sun Yat-Sen University. Since 2019, he has been working as an Associate Professor at the College of Chemistry and Materials Science of Nanjing Normal University. His research interest focuses on synthesis of new crystalline materials (such as POMs, MOFs, COFs and metal-organic clusters) for photo/electrocatalytic applications.

Ya-Qian Lan received his BS and PhD degree (2009) from Northeast Normal University, under the supervision of Prof. Zhong-Min Su. In 2010, he worked as a JSPS postdoctoral fellow at AIST. Since the fall of 2012, he has been a Professor of Chemistry at Nanjing Normal University. His current research interests focus on synthesis of new crystalline materials and catalytic research related to clean energy applications.
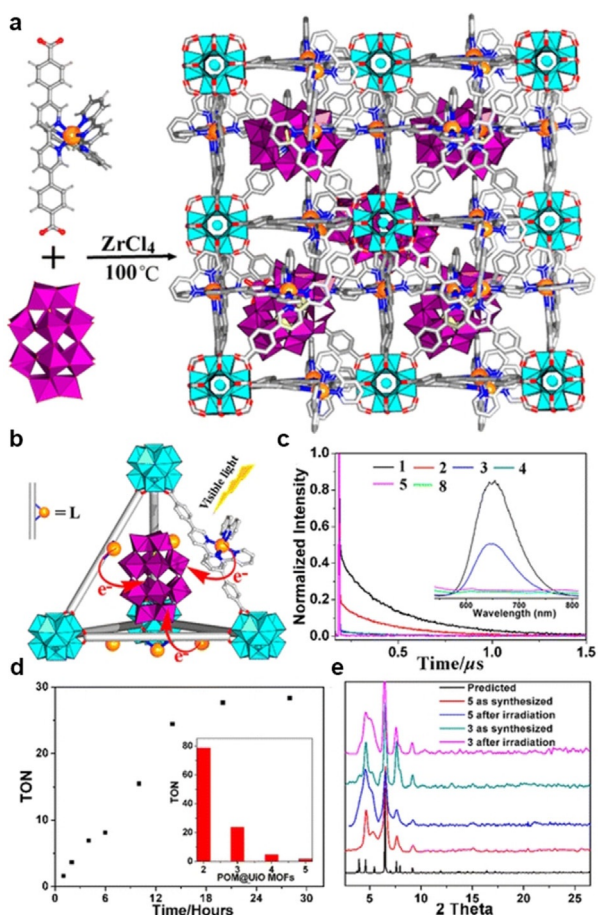
Figure 1. (a) Synthesis of the POM@UiO system via charge-assisted self-assembly. $[P_2W_{18}O_{62}]^{6-}$, purple polyhedra; Zr, cyan; Ru, gold; N, blue; O, red; C, light gray. (b) Schematic showing synergistic visible-light excitation of the UiO framework and multielectron injection into the encapsulated POMs. (c) Decay transients measured at 650 nm ($\lambda_{ex} = 450$ nm) in acidic water (pH 2.0). Inset: Steady-state emission spectra of POM@UiO with $\lambda_{ex} = 450$ nm. (d) Time-dependent HER TONs of POM@UiO-**3** (0.3 mg POM and 6 μL TFA) with methanol as the sacrificial electron donor (inset: TONs of **2–5** after 14 h of HERs). (e) XRD of POM@UiO-**5** (in aqueous solution; 1.5 mg POM and 12 μL TFA) and POM@UiO-**3** (in DMF/CH$_3$CN) before and after photocatalytic reaction. Reproduced from ref. [5b] with permission from American Chemical Society 2015.

semiconductor photochemical properties (HOMO–LUMO transition for POMs) such as photosensitivity. Moreover, POMs due to all-inorganic nature and robust shell topologies exhibit excellent solution, thermal and redox stability, making them attractive homogeneous photocatalysts or catalytic components for HER. In particular, their adjustable redox potential and reversible redox activity are the major advantages of POMs being photocatalysts for HER. For instance, some Keggin-type heteropolytungstates including $PW_{12}O_{40}^{3-}$, $SiW_{12}O_{40}^{4-}$, $BW_{12}O_{40}^{5-}$, $FeW_{12}O_{40}^{5-}$ and $H_2W_{12}O_{40}^{6-}$ have proven to be homogeneous photocatalysts for HER in acidic aqueous solutions under UV-light irradiation.[9] However, traditional POM archetypes often display light absorption in ultraviolet region (large band gap energy), which extremely limits the improvement of photocatalytic efficiency of HER. In this situation, additional photosensitizers (PS) such as noble metal Ru/Ir-based molecular complexes (with visible light response) and noble metal-free metalloporphyrins are chosen to add into reaction system for expanding the light absorption range of POM photocatalyst.[5e,h] Because POMs have remarkable and strong electron acceptability, which makes them effectively receive photo-excited electrons transferred from the LUMO energy level of PS. When the LUMO energy levels of PS are more negative than those of POMs, POMs can serve as electron mediators to accept electrons from PS (this is a spontaneous process). Thus, continuous photo-excited electrons from PS can be transported rapidly to POM catalyst for photocatalytic HER. Simultaneously, the lifetime of photo-generated carriers in PS can be lengthened and the electro-hole pair recombination will be suppressed. In other words, POMs can facilitate the transfer of photo-generated carriers, and thus significantly improving the photocatalytic efficiency of HER. Another sterling characteristic of POMs is that their energy band structure and light absorption range can be adjusted by structure in different valence states. For example, when POMs in their reduced state species (i.e. heteropolyblues, denoted as HPBs), the absorption spectra of some HPBs are likely to have a considerably wide light absorption covering the visible or near infrared region, which will extremely improve the utilization of sunlight to boost the photocatalytic efficiency of HER. Moreover, POMs in reduced state can enrich electrons (electron repositories) relative to their oxidation states and then alter their LUMO and HOMO energy levels, which are very important to the photosensitivity of POMs in reaction process. It was found that the relative energy and composition of the LUMO energy levels of POMs correlated quite well with the electron affinity of each isolated metal ion. Therefore, when a foreign metal or even nonmetal element in different electronegativity is introduced into POM structure, its LUMO energy levels may be changed. This approach can be used to adjust the electronic and/or surface structures of POM-based compound photocatalysts for improving the HER performance.

To date, some Co/Ni/Fe-substituted POM photocatalysts have been reported to provide favorable effects on their HER performance.[5d,10] For example, Hill et al. reported an efficient, robust, and tetra-Ni-substituted molecular POM photocatalyst, $[Ni_4(H_2O)_2(PW_9O_{34})_2]^{10-}$ (Na$_6$K$_4$-**Ni$_4$P$_2$**), which could

potential of H^+/H_2. These two thermodynamic factors are mainly determined by the structural and electronic properties of the semiconductor photocatalyst. Besides, mass diffusion of reactants and products, separation and recombination of photoexcited carriers and the surface HER also have important influences on the efficiency of photocatalytic water splitting. In particular, the charge separation and the surface redox reactions for photocatalyst must proceed within the lifetimes of photoexcited carriers.

Since TiO$_2$ electrodes were first used to perform the photocatalytic splitting of water in 1972,[8] significant progress on exploring metal oxide semiconductor (MOSs) photocatalysts has been made for HER. POMs as a large class of inorganic transition metal oxide cluster polyanions display similar electronic properties to MOSs, and thus possess quasi-

homogeneous catalyze H_2 production over one week and achieved a turnover number (TON) of as high as 6500 with almost no loss in activity with $[Ir(ppy)_2(dtbbpy)][PF_6]$ as photosensitizer and triethanolamine (TEOA) as sacrificial electron donor (for hole consumption).[11] Although homogeneous molecular POM photocatalysts possess a lot of advantages in HER, in some cases their overall negative charge and all-inorganic nature may limit their application scope. As a result, there has been a growing interest in diversifying the photochemical properties of POM molecules by creating hybrid POM- organic/-metal-organic architectures, and thus investigating the effect on modulating photocatalytic HER performance. In recent years, encapsulation of catalytically active POMs in different kinds of porous metal-organic/ inorganic-organic-inorganic/supramolecular organic/ polymeric frameworks (MOFs) which are typically based on electrostatic interactions has been a leading concept for performing enhanced photocatalytic HER.[5b,f–h,12] Lin et al. constructed a charge-assisted hybrid POM@MOF system in which Wells-Dawson $[P_2W_{18}O_{62}]^{6-}$ molecule as the electron acceptor was encapsulated into $[Ru(bpy)_3]^{2+}$-anchored MOF for photocatalytic HER (Figure 1).[5b] As a result of fast multielectron injection from photoactive framework to the encapsulated redox-active $[P_2W_{18}O_{62}]^{6-}$ cluster, an efficient HER performance with TON of 79 was achieved under visible light irradiation. In the same way, they fabricated another Ni_4P_2@MOF system by encapsulating Ni-containing $[Ni_4(H_2O)_2(PW_9O_{34})_2]^{10-}$ molecules into the pores of $[Ir(ppy)_2(bpy)]^+$-anchored phosphorescent UiO-MOFs. Each Ni_4P_2 molecule surrounded closely by multiple $[Ir(ppy)_2(bpy)]^+$ photosensitizers in Ni_4P_2@MOF facilitates a facile multi-electron transfer and then enables efficient visible-light-driven HER with TON as high as 1476. It should be noted that this kind of hybrid approach not only retains the intrinsic redox and structure advantages of POMs but also achieves the heterogenization of molecular POM photocatalyst in HER.

2.2. Water Oxidation

In natural photosynthesis, solar energy-driven water oxidation reaction takes place in the enzyme-cofactor complex Photosystem II (PSII), the highly conserved machinery for the production of plant fuel from sunlight. In this process, P680 (a special chlorophyll dimer) is excited by harvesting photons to generate strong oxidant P680·+, which can oxidize water to dioxygen via the oxygen evolving complex (OEC). Of critical importance is that photosynthetic water oxidation is carried out in a series of proton-coupled electron transfer (PCET) steps. Four protons and four electrons are liberated from two molecules of water molecules to produce one molecule of dioxygen. Water oxidation is catalyzed by a water-oxidizing enzyme (known as OEC) comprised of four manganese ions, one divalent calcium ion, and (probably) chloride. The role of OEC acting as an electrical accumulator in PSII is to couple successive one-electron reductions of P680·+ to four-electron oxidations of water to dioxygen. It is widely accepted that the water oxidation mechanism in PSII occurs though an S-cycle model under-

going five oxidation states of S_0-S_4 transition (Kok cycle).[13] Deep understanding on this photosynthetic mechanism is extremely helpful for the development of artificial water oxidation catalysts (WOCs), because a lot of vital factors including electron-transfer efficiency, oxidizing ability, and the pathway of the O−O bond formation can be inferred from the Kok cycle.[14] However, the water-oxidation is a thermodynamically and kinetically demanding reaction that involves the transfer of four electrons, rearrangement of multiple bonds, and finally O−O bond formation, so it is definitely not easily accomplished in the absence of a WOC catalyst. The basic thermodynamic requirements for the water splitting are associated with a Gibbs free energy (ΔG) of $\approx 237 \text{ kJ mol}^{-1}$, which corresponds to a minimum electrochemical potential of 1.229 V vs. NHE at standard temperature and pressure, suggesting a large overpotential (a deviation from the thermodynamic applied potential) required for operating this reaction. This overpotential translates to a high activation barrier in the context of catalysis. In consideration of such a high oxidation potential, the water oxidation reaction is currently treated as the bottleneck in the development of efficient artificial photosynthetic system and relative applications. Under the circumstances, it is believed that an ideal WOC should be fast, amenable to interfacing with photosensitizing materials, and stable to oxidative, hydrolytic, and thermal degradation during turnover.[14b, 15] In particular, the catalyst with characteristic of synchronizing proton and electron-transfer events is more popular, since the coupling of electron transfer and proton transfer may thus allow the accumulation of multiple redox equivalents, which is an essential requirement in achieving the four-electron oxidation of water.

POMs as a large class of all-inorganic and carbon-free transition metal oxide clusters that show excellent solution, thermal and redox stability in a wide pH range, and has proven to be distinct and attractive photocatalysts for water oxidation. The pH range of thermodynamic stability with respect to hydrolysis and metal oxide formation is determined by the type of POM and its metal composition. In general, "heteropolyanions" including one or more heteroatoms (typically p or d block elements found in one or more positions internal to the polyanion unit) are often stable hydrolytically over wider pH ranges than the "isopolyanions" which contain only the metal and oxygen atoms.[16] Moreover, POMs with metal ions mostly in their highest oxidation states (d^0) can exhibit fast reversible redox transformations under mild conditions, and these redox variations can be modulated over a wide range. Besides, most of POMs bear high negative charges (polyanion) and thus have a commensurate number of counter-cations. When this kind of polyanion cluster exists in aqueous solution, often positively charged PSs (or hydrogen protons) are more likely to be counter-cations to generate POM-photosensitizer complex (POM-PS) (or to surround the POM molecule) due to the ion-pairing effect.[6j,k] Therefore, protons and PSs are easily coupled to the multi-electron transfer of POM photocatalyst to promote the PECT process of water oxidation reaction.

The major breakthrough in the development of POM WOC was achieved in 2008, both of Hill and Bonchio groups

reported a tetra-ruthenium(IV)-substituted POM cluster, $[\{Ru_4O_4(OH)_2(H_2O)_4\}(\gamma\text{-}SiW_{10}O_{36})_2]^{10-}$ (Ru_4SiPOM), which was first used as homogeneous molecular photocatalyst for water oxidation.[17] The Hill group found that a TON of ≈ 18 (corresponding to TOF of 0.45–0.6 s^{-1}) for oxygen evolution can be obtained at pH 7.2, in 20 mM phosphate buffer, and $[Ru(bpy)_3]^{3+}$ was used as the oxidant. Meanwhile, Bonchio group estimated oxygen evolution at pH ≈ 0.6 using excess Ce^{IV} as the oxidant, generating a TON of 500 with an initial TOF of 0.125 s^{-1}. Ru_4SiPOM was shown to catalyze water oxidation under visible light irradiation in the presence of $[Ru(bpy)_3]^{2+}$ and $S_2O_8^{2-}$, which were used as photosensitizer and sacrificial electron acceptor, respectively.[18] Although Ru_4SiPOM undergoes sequential oxidation from Ru^{IV}_4 resting state to the Ru^{V}_4 state, there was no evidence indicated that Ru_4SiPOM WOC is decomposed hydrolytically into the metal oxides (RuO_2, WO_3) under either thermal or photo-driven water oxidation conditions. For the most reported POM WOC, the catalytically active metal centers often not belong to the POM scaffold, which are mainly used as stabilizing units. Santoni et al. reported the first WOC containing only vanadium atoms as catalytically active centers, namely mixed-valence $[(V^{IV}_5V^{V}_1)O_7(OCH_3)_{12}]^-$ species.[19] The catalytically active center in this work is the polyoxometalated framework. The photochemical quantum yield of this POM WOC is estimated to be 0.2 by using $[Ru(bpy)_3]^{2+}$ as the photosensitizer, and $Na_2S_2O_8$ as the sacrificial electron acceptor, in mixed solvents at 450 nm excitation. This result showed that alkoxo-polyoxovanadium clusters are well-suited to take an active part in artificial photosynthetic schemes.

Additionally, inspired by natural oxygenic photosynthesis, oxygen generation occurs at Mn_4O_5Ca moiety and the O—O bond is formed by the cooperation of a multi-redox Mn^{III}/Mn^{IV} manifold, a lot of pristine POM-based photocatalysts as OEC model have been synthesized.[6a,20] Bonchio et al. in 2014 first proposed a POM WOC ($[Mn^{III}_3Mn^{IV}O_3(CH_3COO)_3(A\text{-}\alpha\text{-}SiW_9O_{34})]^{6-}$, denoted as Mn_4POM) including a mixed-valent $Mn^{III}_3Mn^{IV}O_3$ core that mimicked the natural OEC in its reduced S_0 state.[20a] It provides a strategy to access a synthetic Mn_4-OEC by the combination of inorganic POM platform and carboxylate bridges. A defective Mn_4 core featuring mixed valence, multi-redox properties, and photocatalytic behavior was finally obtained by this hybrid set of ligands. The interplay of organic and inorganic ligands provided a coordination environment with both stability and flexibility to assist stepwise one-electron oxidation of the Mn_4-OEC core and to access high-valent Mn states that are responsible for water oxidation. Photocatalytic water oxidation reaction was operated in a buffered medium (pH 5) with a quantum efficiency of 1.7% in the presence of $[Ru(bpy)_3]^{2+}$ and $S_2O_8^{2-}$ (Figure 3). Beyond the homogeneous POM WOC, some approaches are also proposed to fabricate heterogeneous POM WOC photosystems for recyclable utilization, in which POM molecules were immobilized onto/into different supports such as carbon nanodot, g-C_3N_4, graphene, carbon nanotubes, MOFs etc.[6m,n,21] For example, Fontecave and Dolbecq et al. recently reported a stable and easily reusable hybrid POM WOC that immobilizing CoPOM
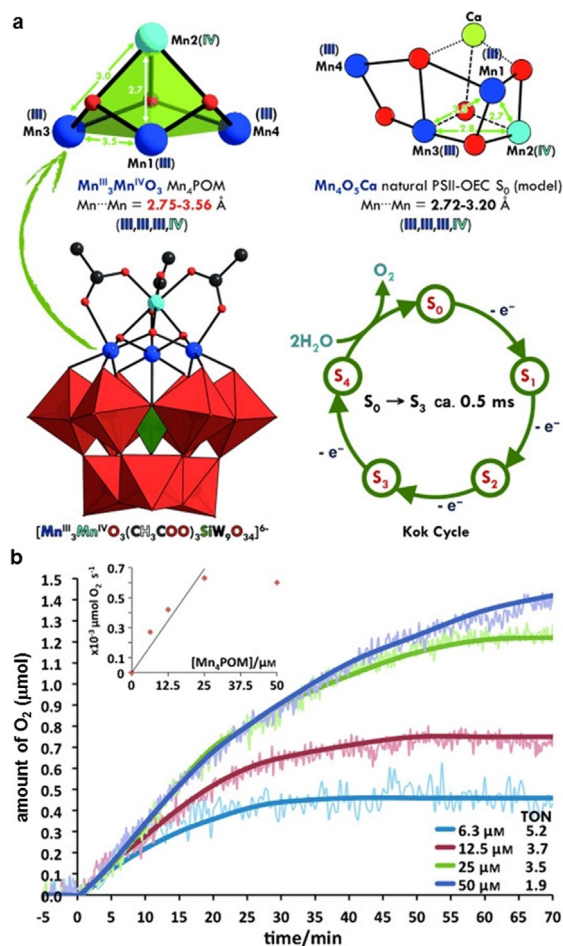

Figure 2. (a) Structural information and Kok cycle. Combined polyhedral/ball-and-stick representation of Mn_4POM (bottom left, counter cations and water molecules in the crystal are not shown for clarity). Comparison of the Mn_4POM core (top left) with the S_0 state of the natural OEC as described by a quantum mechanics/molecular mechanics (QM/MM) model (top right). Photo-induced electron flow within the S_0-S_4 Kok cycle of the natural PSII-OEC (bottom right). (b) Oxygen production upon illumination of a solution containing Mn_4POM (6.3–50 mm), $[Ru(bpy)_3]^{2+}$ (1 mm), and $Na_2S_2O_8$ (5 mm) in $NaHCO_3/Na_2SiF_6$ buffer (50 mm; pH 5.2). Raw data are presented as light traces; smooth, dark lines were added for reasons of clarity. Inset: plot of the initial rate of O_2 production versus the Mn_4POM concentration. Reproduced from ref. [20a] with permission. Copyright 2014, Wiley-VCH.

($[(PW_9O_{34})_2Co_4(H_2O)_2]^{10-}$, $P_2W_{18}Co_4$) into the hexagonal channels of the Zr^{IV} porphyrinic MOF-545.[22] This is a typical supramolecular heterogeneous photocatalytic system with the POM WOC and the photosensitizer within the same host porous solid material. The superior water oxidation performance for $P_2W_{18}Co_4$@MOF-545 photosystem was attributed to two reasons. On the one hand, the porphyrin ligand in MOF can increase the oxidizing power. On the other hand, the confinement of POMs inside the pores of the MOF plays a key role in stabilizing the cobalt POM's catalytic site while the POM-MOF interface provides key components (-OH, labile water molecules) relevant to the OER mechanism.
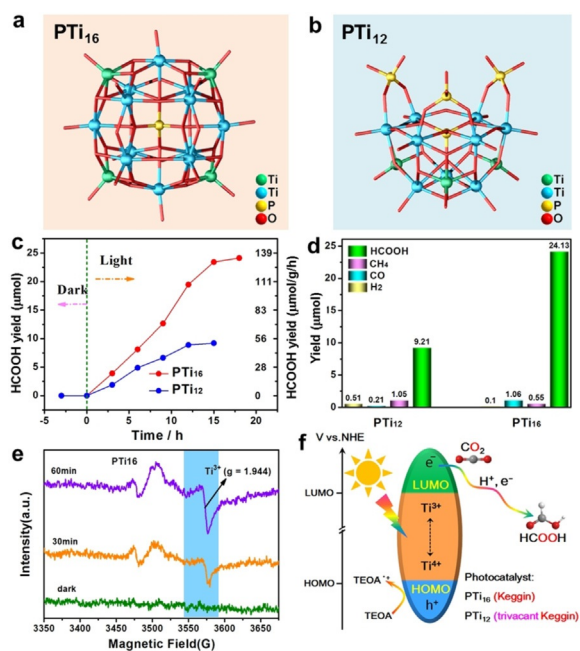
Figure 3. (a,b) Schematic of the heteroatom Keggin structures of PTi$_{16}$ and PTi$_{12}$ and photocatalytic characterizations over **PTi$_{16}$** and **PTi$_{12}$**. (c) Amounts of HCOOH produced as a function of the time of UV light irradiation. (d) The yield distribution of different photocatalytic products. (e) ESR spectra of **PTi$_{16}$**. (f) The proposed reaction mechanism. Reproduced from ref. [26] with permission. Copyright 2019, Wiley-VCH.

2.3. CO$_2$ Reduction

Although massive emission of CO$_2$ has resulted in serious environmental issues, it still is an important non-toxic, highly abundant and cheap carbon feedstock. Photo/electrocatalytic CO$_2$RR represents a favorable means that can reduce CO$_2$ to highly valued hydrocarbon fuels or chemicals by using renewable solar energy or electricity as driving force. For CO$_2$RR, the most important and ambitious goal is to realize the efficient, selective and durable transformation of CO$_2$ into specific product with a view to increasing the possibility of large-scale utilization. However, activation of inert CO$_2$ molecule usually requires a very high energy input because of its high C=O bond dissociation energy (≈ 750 kJ mol^{-1}). Moreover, carbon in CO$_2$ can be reduced from the highest oxidation state to many lower oxidation states, which involves a large variety of reduction products, resulting in that the selectivity of CO$_2$RR is difficult to control. The formation and type of final reduction products is mainly determined by the number of electrons and protons taking part in the reaction. In addition, CO$_2$RR is usually in fierce competition with HER, sometimes partially lowering the efficiency and selectivity towards CO$_2$ conversion. Photocatalytic CO$_2$RR driven by inexhaustible sunlight seems to be a more ideal means compared with electrocatalysis. However, the conversion efficiency, selectivity and stability of the current photocatalyst systems is far from satisfactory, mainly because of the limited active sites, low specific surface area, and fast recombination of the photogenerated electron-hole pairs.[12c,23] To overcome

these drawbacks, highly active photocatalysts should be designed from light harvesting, adsorption of reactants, photo-generated charge separation and transport, and CO$_2$ activation. The catalytic process for CO$_2$RR is very similar to that of photocatalysts for HER, except that the photo-generated electrons in CB or LUMO energy level of photocatalysts are used for CO$_2$RR. The corresponding photo-generated holes after separation are consumed by OER or additional sacrificial electron donors for catalytic cycle. To trigger the photocatalytic CO$_2$RR thermodynamically, the bottom of CB (or LUMO level) of photocatalysts should have a more negative potential than CO$_2$ reduction potentials, and the top of VB (or HOMO level) should be located at a more positive potential than the H$_2$O oxidation potential. The desirable photocatalyst for CO$_2$RR should at least have several characteristics as follow: i) a suitable band gap structure for absorbing photons; ii) an efficient separation and transport of photo-generated electron-hole pairs; iii) plenty of active adsorption and reaction sites for promoting photocatalytic reaction.

POMs as one kind of molecular photocatalysts that display quasi-semiconductor photochemical properties also have many advantages in performing CO$_2$RR, such as superior solution, thermal stability and adjustable redox potential and reversible redox activity, which have also been reflected in photocatalytic HER and OER. Their good solution stability can enable them to carry out photocatalytic CO$_2$RR in water or other solvents, and their own redox properties can assist the multi-electron and multi-proton transfer process required for the conversion of CO$_2$ to products. Despite of the limited light-response range (ultraviolet region), the light absorption of POM photocatalysts can be further improved by many strategies. The most direct and common means is to construct POM-based organic/inorganic frameworks with photosensitive organic ligands or to add auxiliary noble metal photosensitizer into reaction system. However, the catalytically active sites in the reported POM-based photocatalysts are usually foreign metals rather than metal ions in the POM scaffold itself.[7e,f] Of course, the research on CO$_2$RR based on POM-based photocatalysts is still in its infancy, some meaningful conclusions need to be obtained based on more investigations.

In 2010, Neumann and co-workers firstly reported a Ru^{III}-substituted Keggin structure, $\{(C_6H_{13})_4N\}_5[Ru^{III}$-$(H_2O)SiW_{11}O_{39}]$, which catalyzed the photoreduction of CO$_2$ to CO with Et$_3$N as reducing agent.[24] It was demonstrated by DFT calculations that CO$_2$ is preferably coordinated in a side-on manner to Ru^{III} in the POM through formation of a Ru–O bond, further stabilized by the interaction of the electrophilic C atom of CO$_2$ to an O atom of the POM. The interaction of the nucleophilic O atom of CO$_2$ to Ru atom and the formation of a O$_2$C-NMe$_3$ zwitterion stabilize both Ru-O and C-N interactions and probably determine the promotional effect of an amine on the activation of CO$_2$ by POM molecule. Experimental and computed results indicated that the POM takes part in the activation of both CO$_2$ and Et$_3$N. In 2016, Poblet and co-workers studied the photoreduction mechanism of CO$_2$ to CO using a *Re*-organic hybrid POMs $\{NaH[PW_{12}O_{40}]^{3-}$-Re^I**L**-

Angew. Chem. Int. Ed. **2020**, *59*, 20779–20793

© 2020 Wiley-VCH GmbH

www.angewandte.org **20785**

$(CO)_3DMA\}^{n-}$ ($\mathbf{L}$ = 15-crown-5-phenanthroline) via DFT and TD-DFT calculations.[25] In the proposed reaction mechanism, the charge transfer states from POM to *Re* complexes are induced by metal-centered excitations occurring on the reduced POM. The *Re* is responsible for binding and activating CO_2 substrate, while the POM acts as photosensitizer, electron reservoir, as well as electron donor. In 2019, Lan group first reported two Ti^{IV}-based heteroatom Keggin and its trivacant lacunary architectures, $[Ti_{16}$-$(OH)_4O_{20}(PO_4)(OiPr)_{16}]$·guests ($PTi_{16}$, $HOiPr$ = isopropanol) and $[Ti_{12}O_{15}(PO_4)(iPrPO_4)_3$-$(OiPr)_{12}](CHA)_3(H_2O)$ (PTi_{12}, CHA = cyclohexylammonium), both of which can be used as homogeneous photocatalysts for CO_2RR.[26] These photoactive POMs can highly selective reduce CO_2 to HCOOH under ultraviolet irradiation (Figure 3). The Ti^{IV} ions within POM structures are the catalytically active centers for CO_2 reduction, and the generation of Ti^{III} during the photocatalytic process can be detected by electron spin resonance (ESR) measurements. Ti^{4+} ions in POMs were reduced into Ti^{3+} by receiving photo-excited electrons transferred from O^{2-}, while the corresponding photo-generated holes were quenched by sacrificial agent.

Besides, many strategies are used to construct heterogeneous crystalline POM-based photocatalysts for CO_2RR. Recently, Lan group reported several efficient heterogeneous POM-based photocatalyst systems, which can reduce CO_2 to CH_4 with high selectivity and activity. They first synthesized two pure inorganic POM-based frameworks constructed with strong reductive $\{P_4Mo_6^V\}$ units, NENU-605 and NENU-606, both of which can be used as heterogeneous catalysts for photocatalytic CO_2RR.[7a] It should be noted that this is the first POM-based crystalline photocatalysts system to reduce CO_2 to CH_4 in water with a high selectivity of 85.5%. In this work, the strong reductive $\{P_4Mo_6^V\}$ units serving as multi-electron donor played a crucial role in promoting the 8 electrons and 8 protons transfer process required for CO_2-to-CH_4 conversion. To eliminate the participation of additional noble metal PS, Lan group further constructed two POMOFs using reductive Zn-ε-Keggin clusters and photosensitive metalloporphyrin (TCPP) ligands for photocatalytic CO_2RR.[27] The resultant POMOFs successfully achieved the selective photoreduction of CO_2 to CH_4 in water in the absence of any PS, and exhibited very high photocatalytic CH_4 selectivity (> 96%). Notably, the introduction of reductive Zn-ε-Keggin building blocks into POM-based photocatalysts facilitates the photocatalytic selectivity of CH_4 by theoretically delivering adequate electrons to accomplish the 8-electron transfer process of CO_2-to-CH_4 conversion. Moreover, the relevant DFT calculation results also confirmed that the photo-excited electrons more easily flow to POM unit by the efficient bridge effect between reductive Zn-ε-Keggin unit and TCPP linker. These works indicate that assembling strong reducing POM into photocatalyst architecture can increase the possibility of reducing CO_2 to CH_4 or other high-value carbon-based products accompanied with multiple PECT process.

3. POM-based compounds for electrocatalysis

3.1. Hydrogen Production

As a clean and sustainable energy carrier, hydrogen (H_2) shows great potential in addressing energy crisis and improving environmental contamination. It can be produced massively by electrochemical water splitting, which is regarded as one of the most economical and sustainable methods.[28] Of course, electrocatalysts with high efficiency and low cost for the HER is the key to achieving this goal.[29] Although the benchmarking Pt/Pt-based HER electrocatalysts have the best performance, the high cost and low abundance facts severely impede their widespread applications. Thus, the development of highly efficient, stable and inexpensive electrocatalysts for replacing noble metal Pt in HER is imperative and urgent but remains a daunting task. Recently, more and more efforts have been paid on investigating non-noble nanostructured HER electrocatalysts such as transition metal carbides, oxides, phosphides, and sulfides. However, active sites in these electrocatalysts are hard to be controlled effectively by traditional synthetic strategies and the catalysts tend to aggregate under high temperature.

POM-based crystalline materials as electrocatalysts used for HER have drawn more and more attention in the past few decades. Because of the superior redox ability, POM can donate/accept one/more elections reversibly in electrochemical process. This efficient electron transfer provides important prerequisite for POM to be HER electrocatalyst. Besides, POM-based compounds also have many advantages that can be used to construct active non-noble metal-based electrocatalysts and modulate their electrochemical properties, such as i) POM molecule as monodispersed nanocluster is conductive to exposing more catalytically active sites; ii) transition metal (eg. Fe, Co, Ni, etc.)-substituted POM structures can display the synergistic effect between different metal types on improving HER performance; iii) POM molecules can be bridged with organic ligand or confined into pores (host-guest interaction) to form POM-based inorganic-organic hybrid materials with atomically accurate and equally distributed active sites/components; iv) crystalline POM electrocatalysts with well-defined structure help to identify the catalytically active site and study the reaction mechanism. In addition, POM-based electrocatalysts can also be covalently or non-covalently functionalized on different kinds of conductive carbon materials to improve their conductivity, solubility and stability, and then HER performance.

In 2007, Nadjo et al. investigated the activation of POM-based modified electrodes for the HER from acidic aqueous solutions by using different POM molecular catalysts including phosphotungstate $[H_7P_8W_{48}O_{184}]^{33-}$, and Co^{II}-containing silicotungstates $[Co_6(H_2O)_{30}\{Co_9Cl_2(OH)_3(H_2O)_9(\beta$-Si-$W_8O_{31})_3\}]^{5-}$ and $[\{Co_3(B$-β-$SiW_9O_{33}(OH))(B$-β-Si-$W_8O_{29}OH)_2\}_2]^{22-}$. This work highlighted that chemical and physical control of the microenvironment of POM-based modified electrodes can exert remarkable impact on HER performance due to the proton and electron reservoir behaviors of POMs.[30] Of particular note is Cronin's group

made breakthroughs in POM-based water electrolysis systems.[31] A concept of the electron-coupled-proton buffer (ECPB) was introduced by them to design water splitting system ($H_3PMo_{12}O_{40}$ as a redox mediator), by which the production of H_2 and O_2 can achieve separation in space and time. This approach avoids some traditional water electrolysis process issues such as products mixture and electrolyzer degradation. Subsequently, they further used $H_4[SiW_{12}O_{40}]$ as a recyclable redox mediator to build another water splitting system that can prevent gaseous products mixing over a range of current densities and make full use of the precious metal catalysts.[32] Under the effect of the reductive SiW_{12} mediator, the pure H_2 production driven by a platinum-catalyzed system was over 30 times faster than proton exchange membrane electrolyzers at equivalent platinum loading.

Although the reductive POMs have proven to be good electrocatalysts for HER, the large size of their crystals results in that the exposed active site density of the catalyst is greatly reduced. Besides, POMs themselves has low specific area ($< 10\ m^2 g^{-1}$) and high insulativity. Therefore, many efforts have been made to further fixedly load the well-defined POM molecular catalysts onto some excellent conductive substrates such as graphene and carbon nanotube for increasing the active site density, specific area and electron transport capacity.[5i,33] Zhang et al. reported a cyclic 48-tungsto-8-phosphate $[H_7P_8W_{48}O_{184}]^{33-}$ (P_8W_{48}) fixed uniformly in a 3D configuration on reduced graphene oxide sheets (rGO) to boost HER activity.[33] A strong interaction between individual P_8W_{48} and transparent rGO sheets was confirmed by the HRTEM imaging and the solid state ^{31}P NMR spectrum of P_8W_{48}/rGO. Because the rGO nanosheets maintained the high electrical conductivity of the overall electrode, the P_8W_{48}/rGO hybrids finally displayed superior HER activity in acid. It was further confirmed by the reproducible generation of hydrogen with quantitative faradaic yield and a high turnover frequency ($11\ s^{-1}$ at 295 mV overpotential). Significantly, the overpotentials (30 mV at current density of $10\ mA\,cm^{-2}$) for the HER are comparable to those of the commercial Pt/C (20 wt% Pt). In this way, a lot of transition/lanthanide metal-doped POM electrocatalysts deposited on conductive rGO or carbon nanotube have also been shown to afford high HER performance and stability.[34] Most of POMs have significant solubility in reaction medium leading to poor recyclability. Recently, the construction of POMOFs is considered as an effective heterogenization strategy to prevent POMs from dissolving in electrolyte solution.[5a,35] Not only do the POMOFs have high structural modifiability and stability, large surface area and strong confinement effect, but can combine the redox feature of POMs and the porosity of MOFs. Thus, they become more and more attractive in electrocatalytic HER research field. Dolbecq et al. primarily investigated the cation effect on HER activities in XCl (X = Li, Na, K, Cs) media by a POMOF of $(TBA)_3[PMo^V_8Mo^{VI}_4O_{36}(OH)_4Zn_4][C_6H_3(COO)_3]_{4/3}\cdot6H_2O$ ($\varepsilon(trim)_{4/3}$, $TBA^+ = $ tetrabutylammonium ion).[35b] It is worth noting that this is the first report on the non-noble POMOF HER electrocatalyst, which showed a turnover frequency (TOF) as high as ca. $6.7\ s^{-1}$ at the overpotential of 200 mV. In 2015, Lan et al. synthesized two stable {Zn-ε-Keggin}-based

POMOFs, $[TBA]_3[\varepsilon-PMo^V_8Mo^{VI}_4O_{36}(OH)_4Zn_4][BTB]_{4/3}\cdot x$Guest (NENU-500, BTB = benzene tribenzoate) and $[TBA]_3[\varepsilon-PMo^V_8Mo^{VI}_4-O_{37}(OH)_3Zn_4][BPT]$ (NENU-501, BPT = [1,1'-biphenyl]-3,4',5-tricarboxylate).[5a] Both of them showed high structural stability in air as well as tolerance to acidic and basic media, as shown in Figure 4. Because of the effective combination of redox activity of the POM unit and porosity of the MOF, NENU-500 exhibited the highest HER activity among all MOF materials, with a low overpotential of 237 mV at the current density of $10\ mA\,cm^{-2}$. Moreover, the initial electrocatalytic activities of these two POMOFs can still be maintained after 2000 cycles.
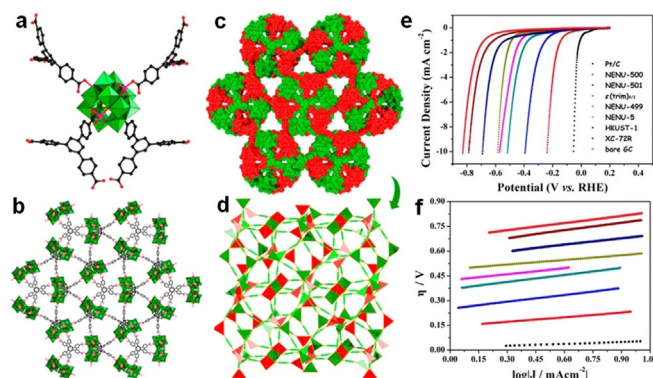

Figure 4. Structural information of NENU-500: (a) connection mode between Zn-ε-Keggin and BTB^{3-} fragments, (b) 3D (3,4)-connected frameworks, (c) two-fold interpenetrated structure, and (d) two-fold interpenetrated **ctn** arrays. Electrochemical characterization of the as-prepared catalysts: (e) polarization curves in 0.5 M H_2SO_4 and (f) corresponding Tafel plots. Reproduced from ref. [5a] with permission. Copyright 2015, American Chemical Society.

3.2. Water Oxidation

Electrochemical water splitting is a two-electrode system composed of HER in the cathode part and OER in the anode part. OER as one half-reaction encompasses the transfer of four electrons and four protons, which requires a higher energy (higher overpotential) than HER to overcome the kinetic barrier for the reaction to occur. Due to the sluggish kinetics, OER is considered to be one of the most important factors to keep electrochemical water splitting system from being of practical use to date.[36] Therefore, development of efficient OER electrocatalysts to improve electrode kinetics and stability under different electrolyte conditions has been paid more attention in the past few decades. In addition, the process of pursuing high-performance electrocatalysts also induces the generation of new techniques that can help to study the properties of materials or the fundamental mechanism of the OER in more detail. Although rutile-type RuO_2 and IrO_2 display excellent OER catalytic activity in both acidic and alkaline electrolytes, their instability under high anodic potential and noble metal nature make them not practical for large-scale utilization. In this situation, substantial research effort has been devoted to exploring and improving the activity of non-noble metal based OER electrocatalysts including nanostructured inorganic or crys-

talline metal-organic coordination materials (such as metal oxides, MOFs and POMs).

POM-based compounds due to rich redox chemistry have been explored as efficient homogeneous/heterogeneous electrocatalysts for OER. In particular, effective combination of different transition metals in the POM-based structures can modulate the redox chemistry and enhance the catalytic activity of the POMs, since transition metals commonly have different oxidation states and coordination geometries (e.g. tetrahedral and octahedral sites), which leads to different activation processes and OER mechanisms. Moreover, if one POM molecule/-based compounds is tuned properly by transition metal, this might result in a low overpotential for it to perform OER. Currently, a series of systematic studies based on transition metal-combined POM electrocatalysts have been reported to offer insightful results that are beneficial to understanding the fundamental mechanism of OER. Additionally, because the inorganic ligands of POMs are difficult to be oxidized during water oxidation process, POM-based compounds and their derived composites thus have been widely used as stable water oxidation catalysts.[37] of course, the electrochemical stability of POM catalysts still needs to be investigated and evidenced more carefully.[6r]

The first POM electrocatalyst for OER, $Na_{14}[Ru^{III}_2Zn_2(H_2O)_2-(ZnW_9O_{34})_2]$, was reported by Shannon and co-workers. The electrochemical generation of O_2 for this di-Ru-substituted POM molecule was investigated on Au electrode using 0.1 M sodium phosphate buffer (pH 8.0) as electrolyte. A Tafel slope of ca. 120 mV was obtained, which is about twice the value typically observed for RuO_2. On the basis of the short Ru-Ru distance (0.318 nm), the authors found that the proximity of the two Ru atoms appears to be a key factor in the electrocatalytic ability to generate O_2.[38] Goberna-Ferron et al. used stable $[Co_9(H_2O)_6(OH)_3(HPO_4)_2(PW_9O_{34})_3]^{16-}$ molecule as true homogeneous catalyst to perform OER.[39] Furthermore, they employed an insoluble $Cs_{15}K[Co_9(H_2O)_6(OH)_3(HPO_4)_2(PW_9O_{34})_3]$ salt to modify amorphous carbon paste electrodes. This heterogeneous catalyst showed a Tafel slope of 148 mV dec^{-1} and remarkable long-term stability in turnover conditions and kept robust catalytic activities in a large pH range.[40]

Just like HER, POM-based compounds as OER electrocatalysts also face the problems of poor stability and conductivity in electrochemical processes. As a result, combining well-defined POMs with all kinds of conductive substrates (e.g. graphene, carbon nanotubes, conductive polymers, nickel foam) to fabricate stable and efficient electrocatalysts for OER has been widely investigated.[6o–q] This approach promotes the heterogenization of POM-based compounds under electrocatalytic conditions and increases the surface area and electron transfer ability of electrocatalytic water splitting cells. The effective electron transfer between POM-based catalyst and conductive substrate is extremely important for the multi-electron transfer OER processes. Especially for the ruthenium with the extensive redox and catalytic chemistry, many Ru-substituted POM molecules have been reported to integrate with conductive substrates to study their OER activities. For example, Prato and co-workers reported very efficient and stable oxygen-

evolving anodes assembled with oxygen-evolving polyoxometalate cluster $(M_{10}[Ru_4(H_2O)_4(\mu-O)_4(\mu-OH)_2(\gamma-Si-W_{10}O_{36})_2]$, M = Cs, Li, denoted as Ru_4POM) and multiwalled carbon nanotubes to address the importance of hybrid interfaces and/or contacts to control and promote electron-transfer events at heterogeneous surfaces.[41] In this way, the OER performance including efficiency, operative voltage, current density and operational stability was improved remarkably. The effective interaction between heterogeneous multiwalled carbon nanotube (MWCNT) support and POM molecules make the resultant POM/MWCNT hybrids displayed controlled material morphology, increased surface area and accelerated sequential electron transferred to the electrode favoring energy dispersion and relieve catalytic fatigue.

In addition, cheap transition metal-containing POM molecular electrocatalysts combined with conductive substrates for OER also have been investigated in past few years. Song and Streb et al. deposited microcrystals of a robust Dexter-Silverton POM molecular catalyst $[Co_{6.8}Ni_{1.2}W_{12}O_{42}(OH)_4(H_2O)_8]$ on macroporous nickel foam electrode by a facile one-step hydrothermal synthesis approach.[42] As shown in Figure 5, The as-fabricated NiCo-POM/Ni electrode showed high OER performance with a low overpotential of 360 mV at 10 mA cm^{-2}, a Tafel slope 126 mV dec^{-1} and a high faradaic efficiency of ≈96% in an alkaline aqueous solution (pH 13). It is noted that this electrode is the first stable POM-

Figure 5. Deposition of Dexter-Silverton polyoxometalate microcrystals on nickel foam electrodes (*Top*). (a) IR-corrected polarization curves in 0.1 M KOH at 5 mVs^{-1}. (b) Tafel plots of Ni foam and the NiCo-POM/Ni electrode. (c) SEM image of NiCo-POM/Ni electrode after stability test over 10 h OER; (d) PXRD spectra of NiCo-POM/Ni before and after stability test over 10 h OER. Reproduced from ref. [42] with permission. Copyright 2017, Wiley-VCH.

based OER system for use in alkaline water electrolysers, because it can operate for prolonged periods of time under basic conditions without chemical or mechanical degradation and no physical detachment. Moreover, the post-catalytic analyses results indicated that the morphology and crystal structure of POM catalyst were unchanged, highlighting its stability under basic and oxidizing conditions. In 2018, Galan-Mascaros group reported water-insoluble Co-POM salts with cesium or barium counter-cations to study their OER performance in acidic media.[43] Ba[Co-POM] in this work showed the excellent and unparalleled OER performance with an overpotential of 189 mV vs. RHE at 1 mA cm^{-2}, which outperformed the state-of-the-art IrO$_2$ catalyst even in an acidic electrolyte (pH < 1). From the significance influence of barium dications in the activity of the [Co-POM], the POMs afford an intrinsic advantage, because their polyanionic nature made them easy to selectively incorporate the desired ancillary counter-cations close to their active sites, without structurally or chemically affecting their appropriate environment. Additionally, they found that a carbon-paste conducting support with a hydrocarbon binder could improve the stability of metal-oxide catalysts in acidic media by providing a hydrophobic environment.

3.3. CO$_2$ Reduction

The massive emission of CO$_2$ derived from the fossil fuels burning into the atmosphere has triggered severe environmental and energy issues. Reducing CO$_2$ into value-added fuels (such as C$_2$H$_4$, CH$_4$, CO) or chemicals (such as HCOOH, CH$_3$OH, C$_2$H$_5$OH) is one of the promising paths to address these issues and affords a convenient solution for energy conversion. Compared with the photocatalytic CO$_2$ reduction, electrical energy-driven CO$_2$ reduction is also an effective technology to realize this reaction process and commonly shows higher conversion efficiency. Likewise, the target products for electrochemical CO$_2$RR are obtained by proton-coupled multiple-electron (2, 6, 8, or 12 electrons) transfer mechanism, and often classified into mono-carbon (C$_1$) and multi-carbon (C$_n \geq 2$) reductive products. In view of the higher energy density, selective and efficient synthesis of C$_n$ products by electrochemical CO$_2$RR is more favorable than C$_1$ products. However, HER as a competitive reaction in aqueous electrolytes in most cases extremely reduces the conversion efficiency of CO$_2$ during the electrochemical process, because it can occur at a comparable thermodynamic potential to that of CO$_2$RR. Besides, HER-triggered side reactions also can degrade the performance of CO$_2$RR. In this regard, the search of superior electrocatalysts with excellent electrochemical activity and suppressive HER is of great importance to the development of CO$_2$RR.

In the past few decades, many efforts have been devoted to the exploration and design of efficient homogeneous or heterogeneous catalysts for electrocatalytic CO$_2$RR by using various novel electrode materials. In general, the desirable electrocatalysts for CO$_2$RR should be constructed with the following fundamental features: i) flexible redox ability for the multielectron transfer, ii) high Faradaic efficiency and selectivity for the CO$_2$RR, iii) high structural and performance stability during a long-term electrochemical process, iv) high catalytic activity with a low electrochemical overpotential, and v) scalable synthesis from low cost raw materials. At present, the most reported heterogeneous elelctrocatalysts for CO$_2$RR mainly focus on nanostructured materials, while the contrary homogeneous elelctrocatalysts mainly involve molecular metal complexes and macrocyclic organics.

POM-based compounds due to their intrinsic proton- and electron-storage properties can serve as attractive homogeneous or heterogeneous electrocatalysts to promote the multielectron reduction of CO$_2$ to useful chemicals. Moreover, POMs as weak bases could promote the formation of hydrogen-bond networks in the vicinity of the CO$_2$ coordination center to favor proton-coupled electron transfer that occurs when the proton source is close to the catalytically active center.[44] In particular, transition-metal-substituted POM molecules that is likely to fix or react with CO$_2$ to form reversible complexes, which seems to be beneficial for photo/electrocatalytic CO$_2$RR, as demonstrated by the works of Kozik *et.al.*[45] On this foundation, the first POM electrocatalyst used for multiproton-multielectron CO$_2$RR, (TOA)$_6$[α-SiW$_{11}$O$_{39}$Co(_)] (TOA = tetraoctyl ammonium; _ = vacant position in the coordination sphere of Co), was studied by Proust group in homogeneous solution.[46] In this work, the use of POM molecule can promotes the electrocatalytic reduction of CO$_2$ to CO in CO$_2$-saturated dichloromethane solution and further reduction of CO to more valuable formaldehyde by performing the four-electron/four-proton transfer mechanism. Because no H$_2$ production was detected during electrolysis at various timescales, thus this catalyst displayed a high selectivity for CO$_2$ reduction. Meanwhile, the system appears to be quite robust in consideration of its continuous activity for more than 66 h electrolysis, yielding a TON of 3.7. Despite of the low faradic yield, this POM molecule shows the great potential to selectively promote the electrocatalytic reduction of CO$_2$ to CO or even the four-electron/four-proton reduction product of formaldehyde.

Besides, soluble POM molecules can be assembled with organic ligands to construct stable metal-cluster organic framework materials, which are treated as heterogeneous electrocatalysts to perform CO$_2$RR. In 2018, Lan et al. first developed a serious of stable and precisely designed crystalline POM-based organic frameworks (M-PMOFs, M = Co, Fe, Ni, Zn) to study electrocatalytic CO$_2$RR.[7b] For these structures, reductive {ε-PMo$_8^V$Mo$_4^{VI}$O$_{40}$Zn$_4$} cluster and metalloporphyrin ligand were used as building block and linker, respectively. The effective combination of electron-donating POM unit and active metalloporphyrin under the exertion of the electric field generate an oriented electronic transportation channel that is helpful for the accomplishment of multiple electrons transfer process in electrocatalytic CO$_2$RR. As shown in Figure 6, the Co-PMOF among these electrocatalysts exhibited selective CO$_2$-to-CO reduction performance with a faradaic efficiency of 94% over a wide potential range (−0.8 to −1.0 V). Moreover, its best faradaic efficiency can reach up to 99% (highest in reported metal-organic
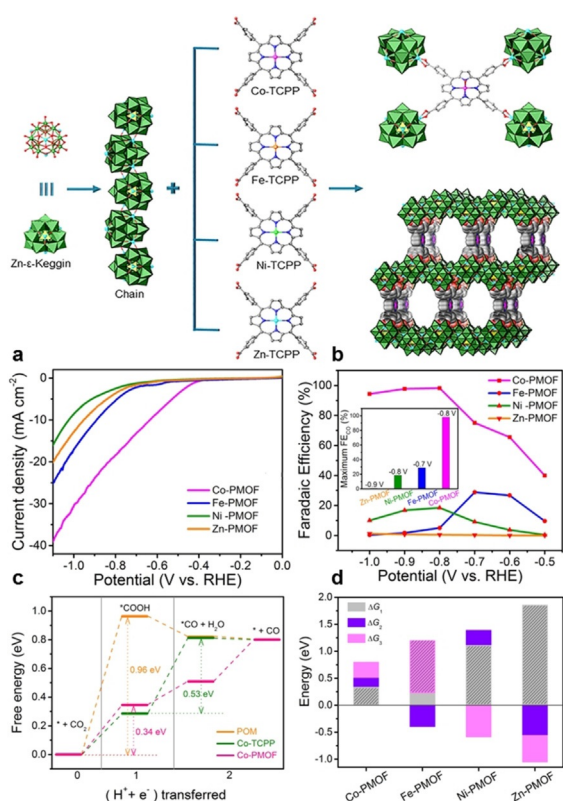
Figure 6. Schematic illustration of the structures of M-PMOFs (M = Co, Fe, Ni, Zn) (*Top*). (a) Linear sweep voltammetric curves. (b) Faradaic efficiencies for CO. (c) The free energy diagrams of CO_2 reduction to CO by DFT calculation. (d) Comparison of the free energy of each elementary reaction (ΔG_1, ΔG_2, and ΔG_3 represent the free energy of *COOH formation, *CO formation, and CO desorption process, respectively) in CO_2 RR. Reproduced from ref. [7b] with permission. Copyright 2018, Nature Publishing Group.

frameworks) along with a high TOF of 1656 h^{-1} and good catalysis durability (> 36 h). The corresponding DFT calculation results based on crystal structure model indicated that the efficiently synergistic electron modulation of Zn-ε-Keggin and Co-TCPP possesses remarkably reduced free energies for the adsorbed intermediates (*COOH and *CO) formation compared with single components, and particularly the rate-determining steps of *COOH formation decrease to a much smaller free energy of $\Delta G_1 = 0.34$ eV, being consistent with the obtained high electroreduction activity and selectivity. Additionally, these results also indicated that the favorable active site for CO_2RR is the Co ion in TCPP pocket instead of POM unit. However, due to the large size, these crystalline PMOFs need to be carefully ground before electrode preparation. At present, report on POMs for CO_2 electroreduction is still scarce. Although POM molecule, PMOF and nanocomposite (such as Ag-PMo[7h]) have been applied to this reaction, only CO as the main reductive product is obtained. Therefore, designing and synthesizing more effective POM-based electrocatalysts to obtain value-added multi-carbon products still needs further exploration.

4. Conclusions and Outlook

4.1. Advantages

POM-based compounds have displayed outstanding advantages in photo/electrocatalytic HER, OER and CO_2RR, owing to their intrinsic and tunable solution, thermal and redox stability, semiconductor-like behaviour and acidity. Moreover, their polyanions nature and stable polymetallic valence tautomerism can greatly promote the PCET process required for the formation of oxidation and reduction products. Additionally, the reductive POM structures (or POMs with low oxidation states) appear to display significant advantages in HER and CO_2RR, especially for the generation of products with multi-electron and multi-proton transfer in photocatalytic CO_2RR. The reported synthetic methodologies of efficient and stable POM-based photo/electrocatalysts can be classified into four strategies as follow: i) constructing high nuclearity POMs assembled with several polyanion units or foreign metal/central heteroatom substituted POMs to realize the controllable electronic structure and vigorous electron transfer, ii) introducing different numbers of catalytically active sites into POMs to prepare single-site or single-cluster catalysts, iii) incorporating POM molecules into porous materials to achieve heterogenization and input redox capability, iv) integrating POMs to different kinds of conductive substrates to improve the electronic conductivity and reduce its dissolution in aqueous solutions.

4.2. Challenges

Some progress has been made in the fields of photo/electrocatalytic HER, OER and CO_2RR by using POM-based compounds as catalysts, but there are still some problems that need to be further resolved and improved. First, soluble POM molecules usually serve as homogeneous photo/electrocatalysts, but the development of heterogeneity strategies is still limited in consideration of the practical application and product separation in future. Although POM molecules can be deposited on various conductive substrates to achieve heterogenization and improve the conductivity of the catalyst, these multi-phase hybrid catalysts due to extensive vacancies, insufficient structure information, complex active ingredients, etc. are difficult to be accurately determined the corresponding structure-property relationship. Secondly, the catalytic activity of metal sites in traditional POM-based clusters is poor due to their saturated coordination sphere. Thirdly, most reported heterogeneous POM-based photo/electrocatalysts exhibit an obvious reduction in catalytic activity with the prolongation of the reaction time, indicating their unsatisfactory structural stability under the conditions of prolonged photo-corrosion, stirring process, and alkaline sacrificial corrosion. Fourth, the very limited results that have been reported fail to show how specific types of POM structures affect their photo/electrocatalytic performance. Besides, the mechanism that studies the influences of polymetallic/heterometallic synergistic effect in POM scaf-

fold on production of different CO_2 reduction products is still lacking.

For photocatalytic reactions, the limited light absorption ability and heterogenization of crystalline POM-based photocatalysts still need to be greatly improved, because most of the reported POM molecules are homogeneous catalysts and require additional photosensitizers and/or sacrificial agents to maintain the catalytic reaction cycle. For the green catalytic reaction itself, the significance is greatly weakened, so it is necessary to find more desirable solutions. For electrocatalytic reactions, POM-based compounds face many severe problems including i) poor electronic conductivity (most of POM assemblies are insulating), ii) limited structural stability under electrocatalytic conditions, iii) the large crystal size of POM-based compounds needs to be grinded to prepare the electrode and iv) limited number of exposed active site, etc. In addition, although POM-based catalysts have been applied to CO_2 electroreduction, the reductive products are still limited to CO with 2 electrons and 2 protons transfer. How to design and synthesize more efficient POM-based electrocatalysts to obtain value-added multi-carbon products still needs further exploration. Of course, according to the structure and performance characteristics of the POM electrocatalyst, further improvement of the electrocatalytic device also might be beneficial and important.

4.3. Strategies

It is obvious that the structural stability and electrical conductivity of POM-based compounds are the most fundamental and important requirements in their photo/electrocatalytic applications. In order to effectively increase the structural stability and conductivity of POM-based compounds, the following strategies can be considered: i) Introduction of the coordination effect or protection of functionalized organic ligands (such as hydrophobic, conductive groups modification etc.) can regulate the inherent physical and chemical properties of POM-based compounds. Moreover, the efficient electron transfer between POM and organic ligand sometimes can extend the light absorption of POM-based compounds, which is conductive to improving photocatalytic performance. ii) In addition to considering further strengthening the bonding strength of POM-based compounds and conductive substrates, building a good conductivity transfer mode (such as the classic -M-N-N-M-bridging mode, etc.) in the structure may be also helpful for increasing the intrinsic electrical conductivity of compound. It is well known that metal sites in traditional POM-based clusters display the poor catalytic activity because of their saturated coordination sphere. Moreover, their structures lack specific active sites for oxidation and/or reduction reactions, which results in their inability to complete a single or cooperative output of stable oxidation and/or reduction catalytic activity. By specifically designing the coordination geometry of metal sites with more flexible structural assembly strategies and functionalized organic ligand selection, their catalytic activity can be effectively releasing. This method can also introduce specific oxidation and/or reduction metal

catalytic active centers by selecting different high and low oxidation state metal sources in the process of structure assembly. Last but not least, the reported heterogeneous POM-based compounds photo/electrocatalysts always have large crystal size. Although more catalytically active sites can be exposed after effective grinding, the crystal morphology is also greatly damaged and more structural defects are exposed to affect the assessment of catalytic reaction activity. In this regard, appropriate adjustments/ interventions (such as adding effective regulators, reducing the growth time of crystal nuclei, etc.) in the structural assembly process of POM-based compounds can be used to prepare nano- or micro-nano crystals, which can increase the number of active sites exposed on the catalyst surface per unit mass.

4.4. Outlooks

The tunable redox properties and fast electron transfer of POM-based compounds are closely related to the variations on their electronic and geometric structure, which is critical in photo/electrocatalytic processes. On this basis, to give a picture on how to rationally design more promising POM-based photo/electrocatalysts applied for efficient HER, OER and CO_2RR, many aspects of research can be further advanced in the future. i) While making full use of inherent characteristics, the structural stability and electronic conductivity of POM-based crystalline materials should be greatly improved through more effective synthesis strategies or preparation processes of POM assemblies, especially under electrocatalytic conditions. This is the basic condition for judging and explaining the mechanism of photo/electrocatalytic reaction mechanism based on the POM-containing compound structure. ii) Considering the tunable redox state of POMs, the assembly (or encapsulation) of reductive POM building blocks (or guests) into the structure of photo/electrocatalyst may be an effective strategy for obtaining high-value reductive products in photo/electrocatalytic CO_2RR. Moreover, construction of efficient POM-based photo/electrocatalysts configured with precisely catalytic active site to reduce CO_2 to specific products selectively and durably is of great importance. iii) The in situ photo/electrochemical characterizations or devices should be developed to monitor the dynamically structural changes of POM-based compound during the photo/electrocatalytic reaction process and then uncover the real catalytic reaction mechanism. iv) For the photocatalytic CO_2RR, it is a big goal to realize the artificial photosynthesis overall reaction (i.e. combination of CO_2 photoreduction and H_2O photooxidation reactions without help of additional photosensitizer and sacrificial agent) in H_2O through functionalized structural modification of POM-based photocatalysts. The most difficult and important thing is how to achieve the coexistence and cooperativity of oxidative and reductive active sites in one POM-based photocatalyst structure. In addition, it is also important to develop more POM-based photo/electrocatalysts with intrinsically catalytic activity from the constituted metals rather than foreign metals.

Finally, we hope that the summary of advantages, challenges, strategies, and outlooks (Figure 7) of POM-based
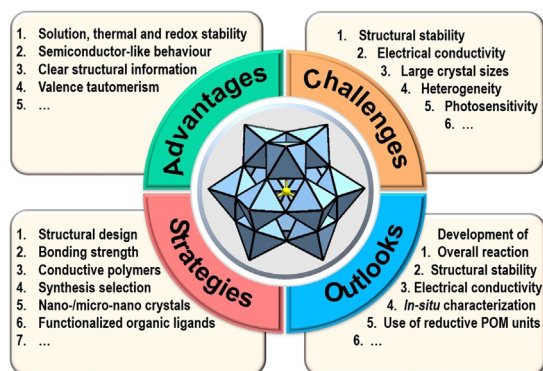
Figure 7. Schematic illustration of advantages, challenges, strategies and outlooks of the well-defined POM-based compounds in photo/electrocatalytic applications.

compounds in photo/electrocatalytic applications can provide a lot of insights and opportunities to further improve their catalytic performance.

Conflict of interest

The authors declare no conflict of interest.

[1] T. Sakakura, J.-C. Choi, H. Yasuda, *Chem. Rev.* **2007**, *107*, 2365 – 2387.

[2] a) X. Chang, T. Wang, J. Gong, *Energy Environ. Sci.* **2016**, *9*, 2177 – 2196; b) S. Berardi, S. Drouet, L. Francas, C. Gimbert-Surinach, M. Guttentag, C. Richmond, T. Stoll, A. Llobet, *Chem. Soc. Rev.* **2014**, *43*, 7501 – 7519.

[3] a) D.-Y. Du, J.-S. Qin, S.-L. Li, Z.-M. Su, Y.-Q. Lan, *Chem. Soc. Rev.* **2014**, *43*, 4615 – 4632; b) N. M. Haralampos, J. Yan, D. L. Long, L. Cronin, *Chem. Soc. Rev.* **2012**, *41*, 7403 – 7430; c) J. J. Walsh, A. M. Bond, R. J. Forster, T. E. Keyes, *Coord. Chem. Rev.* **2016**, *306*, 217 – 234.

[4] a) X.-X. Li, D. Zhao, S.-T. Zheng, *Coord. Chem. Rev.* **2019**, *397*, 220 – 240; b) H. N. Miras, L. Vilà-Nadal, L. Cronin, *Chem. Soc. Rev.* **2014**, *43*, 5679 – 5699.

[5] a) J.-S. Qin, D.-Y. Du, W. Guan, X.-J. Bo, Y.-F. Li, L.-P. Guo, Z.-M. Su, Y.-Y. Wang, Y.-Q. Lan, H.-C. Zhou, *J. Am. Chem. Soc.* **2015**, *137*, 7169 – 7177; b) Z.-M. Zhang, T. Zhang, C. Wang, Z. Lin, L.-S. Long, W. Lin, *J. Am. Chem. Soc.* **2015**, *137*, 3197 – 3200; c) C. Freire, D. M. Fernandes, M. Nunes, V. K. Abdelkader, *ChemCatChem* **2018**, *10*, 1703 – 1730; d) R. Liu, X. Shang, C. Li, X. Xing, X. Yu, G. Zhang, S. Zhang, H. Cao, L. Bi, *Int. J. Hydrogen Energy* **2013**, *38*, 9954 – 9960; e) A. Panagiotopoulos, A. M. Douvas, P. Argitis, A. G. Coutsolelos, *ChemSusChem* **2016**, *9*, 3213 – 3219; f) R. Prabu, K. Peramaiah, N. Palanisami, P. P. Pescarmona, B. Neppolian, S. Shanmugan, *Inorg. Chem.*

Front. **2018**, *5*, 2666 – 2677; g) D. Shi, R. Zheng, C.-S. Liu, D.-M. Chen, J. Zhao, M. Du, *Inorg. Chem.* **2019**, *58*, 7229 – 7235; h) S.-B. Yu, Q. Qi, B. Yang, H. Wang, D.-W. Zhang, Y. Liu, Z.-T. Li, *Small* **2018**, *14*, 1801037; i) W. Xu, C. Liu, W. Xing, T. Lu, *Electrochem. Commun.* **2007**, *9*, 180 – 184.

[6] a) X.-B. Han, Y.-G. Li, Z.-M. Zhang, H.-Q. Tan, Y. Lu, E.-B. Wang, *J. Am. Chem. Soc.* **2015**, *137*, 5486 – 5493; b) Q. Yin, J. M. Tan, C. Besson, Y. V. Geletii, D. G. Musaev, A. E. Kuznetsov, Z. Luo, K. I. Hardcastle, C. L. Hill, *Science* **2010**, *328*, 342 – 345; c) V. K. Abdelkader-Fernández, D. M. Fernandes, S. S. Balula, L. Cunha-Silva, C. Freire, *ACS Appl. Energy Mater.* **2020**, *3*, 2925 – 2934; d) F. Song, Y. Ding, B. Ma, C. Wang, Q. Wang, X. Du, S. Fua, J. Song, *Energy Environ. Sci.* **2013**, *6*, 1170 – 1184; e) X. Du, Y. Ding, F. Song, B. Ma, J. Zhao, J. Song, *Chem. Commun.* **2015**, *51*, 13925 – 13928; f) L. Yu, X. Du, Y. Ding, H. Chen, P. Zhou, *Chem. Commun.* **2015**, *51*, 17443 – 17446; g) Z. Han, A. M. Bond, C. Zhao, *Sci. China Chem.* **2011**, *54*, 1877 – 1887; h) L. L. Tinker, N. D. McDaniel, S. Bernhard, *J. Mater. Chem.* **2009**, *19*, 3328 – 3337; i) T. Ueda, *ChemElectroChem* **2018**, *5*, 823 – 838; j) P.-E. Car, M. Guttentag, K. K. Baldridge, R. Alberto, G. R. Patzke, *Green Chem.* **2012**, *14*, 1680 – 1688; k) F. Evangelisti, P.-E. Car, O. Blacque, G. R. Patzke, *Catal. Sci. Technol.* **2013**, *3*, 3117 – 3129; l) B. Chakraborty, G. Gan-Or, Y. Duan, M. Raula, I. A. Weinstock, *Angew. Chem. Int. Ed.* **2019**, *58*, 6584 – 6589; *Angew. Chem.* **2019**, *131*, 6656 – 6661; m) Y. Choi, D. Jeon, Y. Choi, J. Ryu, B.-S. Kim, *ACS Appl. Mater. Interfaces* **2018**, *10*, 13434 – 13441; n) J. Zhou, W. Chen, C. Sun, L. Han, C. Qin, M. Chen, X. Wang, E. Wang, Z. Su, *ACS Appl. Mater. Interfaces* **2017**, *9*, 11689 – 11695; o) M. Blasco-Ahicart, J. Soriano-López, J. R. Galán-Mascarós, *ChemElectroChem* **2017**, *4*, 3296 – 3301; p) G. Y. Lee, I. Kim, J. Lim, M. Y. Yang, D. S. Choi, Y. Gu, Y. Oh, S. H. Kang, Y. S. Nam, S. O. Kim, *J. Mater. Chem. A* **2017**, *5*, 1941 – 1947; q) M. Quintana, A. M. López, S. Rapino, F. M. Toma, M. Iurlo, M. Carraro, A. Sartorel, C. Maccato, X. Ke, C. Bittencourt, T. Da Ros, G. Van Tendeloo, M. Marcaccio, F. Paolucci, M. Prato, M. Bonchio, *ACS Nano* **2013**, *7*, 811 – 817; r) S. J. Folkman, R. G. Finke, *ACS Catal.* **2017**, *7*, 7 – 16.

[7] a) S.-L. Xie, J. Liu, L.-Z. Dong, S.-L. Li, Y.-Q. Lan, Z.-M. Su, *Chem. Sci.* **2019**, *10*, 185 – 190; b) Y.-R. Wang, Q. Huang, C.-T. He, Y. Chen, J. Liu, F.-C. Shen, Y.-Q. Lan, *Nat. Commun.* **2018**, *9*, 4466; c) S. Barman, S. S. Sreejith, S. Garai, R. Pochamoni, S. Roy, *ChemPhotoChem* **2019**, *3*, 93 – 100; d) S. Das, T. Balaraju, S. Barman, S. S. Sreejith, R. Pochamoni, S. Roy, *Front. Chem.* **2018**, *6*, 514; e) J. Ettedgui, Y. Diskin-Posner, L. Weiner, R. Neumann, *J. Am. Chem. Soc.* **2011**, *133*, 188 – 190; f) E. Haviv, L. J. W. Shimon, R. Neumann, *Chem. Eur. J.* **2017**, *23*, 92 – 95; g) S.-M. Liu, Z. Zhang, X. Li, H. Jia, M. Ren, S. Liu, *Adv. Mater. Interfaces* **2018**, *5*, 1801062; h) S.-X. Guo, F. Li, L. Chen, D. R. MacFarlane, J. Zhang, *ACS Appl. Mater. Interfaces* **2018**, *10*, 12690 – 12697.

[8] A. Fujishima, K. Honda, *Nature* **1972**, *238*, 37 – 38.

[9] a) H. Hori, K. Koike, Y. Sakai, H. Murakami, K. Hayashi, K. Nomiya, *Energy Fuels* **2005**, *19*, 2209 – 2213; b) T. Yamase, R. Watanabe, *J. Chem. Soc. Dalton Trans.* **1986**, 1669 – 1675.

[10] a) H. Lv, Y. Chi, P. van Leusen, P. Kögerler, Z. Chen, J. Bacsa, Y. V. Geletii, W. Guo, T. Lian, C. L. Hill, *Chem. Eur. J.* **2015**, *21*, 17363 – 17370; b) V. Singh, Z. Chen, P. Ma, D. Zhang, M. G. B. Drew, J. Niu, J. Wang, *Chem. Eur. J.* **2016**, *22*, 10983 – 10989.

[11] H. Lv, W. Guo, K. Wu, Z. Chen, J. Bacsa, D. G. Musaev, Y. V. Geletii, S. M. Lauinger, T. Lian, C. L. Hill, *J. Am. Chem. Soc.* **2014**, *136*, 14015 – 14018.

[12] a) E. D. Koutsouroubi, I. T. Papadas, G. S. Armatas, *ChemPlusChem* **2016**, *81*, 947 – 954; b) J. Tian, Z.-Y. Xu, D.-W. Zhang, H. Wang, S.-H. Xie, D.-W. Xu, Y.-H. Ren, H. Wang, Y. Liu, Z.-T. Li, *Nat. Commun.* **2016**, *7*, 11580; c) X. F. Li, S. B. Yu, S. Yang, J. Tian, H. Wang, D. W. Zhang, Y. Liu, Z. T. Li, *Sci. China Chem.*

2018, *61*, 830–835; d) X.-J. Kong, Z. Lin, Z.-M. Zhang, T. Zhang, W. Lin, *Angew. Chem. Int. Ed.* **2016**, *55*, 6411–6416; *Angew. Chem.* **2016**, *128*, 6521–6526.

[13] a) G. Renger, T. Renger, *Photosynth. Res.* **2008**, *98*, 53–80; b) M. Haumann, P. Liebisch, C. Müller, M. Barra, M. Grabolle, H. Dau, *Science* **2005**, *310*, 1019–1021.

[14] a) S. Romain, L. Vigara, A. Llobet, *Acc. Chem. Res.* **2009**, *42*, 1944–1953; b) M. D. Kärkäs, O. Verho, E. V. Johnston, B. Åkermark, *Chem. Rev.* **2014**, *114*, 11863–12001.

[15] H. Inoue, T. Shimada, Y. Kou, Y. Nabetani, D. Masui, S. Takagi, H. Tachibana, *ChemSusChem* **2011**, *4*, 173–179.

[16] H. J. Lv, Y. V. Geletii, C. C. Zhao, J. W. Vickers, G. B. Zhu, Z. Luo, J. Song, T. Q. Lian, G. D. Musaev, L. C. Hill, *Chem. Soc. Rev.* **2012**, *41*, 7572–7589.

[17] a) Y. V. Geletii, B. Botar, P. Kögerler, D. A. Hillesheim, D. G. Musaev, C. L. Hill, *Angew. Chem. Int. Ed.* **2008**, *47*, 3896–3899; *Angew. Chem.* **2008**, *120*, 3960–3963; b) A. Sartorel, M. Carraro, G. Scorrano, R. D. Zorzi, S. Geremia, N. D. McDaniel, S. Bernhard, M. Bonchio, *J. Am. Chem. Soc.* **2008**, *130*, 5006–5007.

[18] Y. V. Geletii, Z. Huang, Y. Hou, D. G. Musaev, T. Lian, C. L. Hill, *J. Am. Chem. Soc.* **2009**, *131*, 7522–7523.

[19] M.-P. Santoni, G. La Ganga, V. Mollica Nardo, M. Natali, F. Puntoriero, F. Scandola, S. Campagna, *J. Am. Chem. Soc.* **2014**, *136*, 8189–8192.

[20] a) R. Al-Oweini, A. Sartorel, B. S. Bassil, M. Natali, S. Berardi, F. Scandola, U. Kortz, M. Bonchio, *Angew. Chem. Int. Ed.* **2014**, *53*, 11182–11185; *Angew. Chem.* **2014**, *126*, 11364–11367; b) B. Schwarz, J. Forster, M. K. Goetz, D. Yücel, C. Berger, T. Jacob, C. Streb, *Angew. Chem. Int. Ed.* **2016**, *55*, 6329–6333; *Angew. Chem.* **2016**, *128*, 6437–6441; c) Q. Xu, H. Li, L. Chi, L. Zhang, Z. Wan, Y. Ding, J. Wang, *Appl. Catal. B* **2017**, *202*, 397–403; d) X.-B. Han, Z.-M. Zhang, T. Zhang, Y.-G. Li, W. Lin, W. You, Z.-M. Su, E.-B. Wang, *J. Am. Chem. Soc.* **2014**, *136*, 5359–5366.

[21] a) D. Zhou, B.-H. Han, *Adv. Funct. Mater.* **2010**, *20*, 2717–2722; b) W. A. Shah, A. Waseem, M. A. Nadeem, P. Kögerler, *Appl. Catal. A* **2018**, *567*, 132–138; c) L. Xi, Q. Zhang, Z. Sun, C. Song, L. Xu, *ChemElectroChem* **2018**, *5*, 2534–2541; d) Q. Lan, Z.-M. Zhang, C. Qin, X.-L. Wang, Y.-G. Li, H.-Q. Tan, E.-B. Wang, *Chem. Eur. J.* **2016**, *22*, 15513–15520.

[22] G. Paille, M. Gomez-Mingot, C. Roch-Marchal, B. Lassalle-Kaiser, P. Mialane, M. Fontecave, C. Mellot-Draznieks, A. Dolbecq, *J. Am. Chem. Soc.* **2018**, *140*, 3613–3618.

[23] W. Tu, Y. Zhou, Z. Zou, *Adv. Mater.* **2014**, *26*, 4607–4626.

[24] A. M. Khenkin, I. Efremenko, L. Weiner, J. M. L. Martin, R. Neumann, *Chem. Eur. J.* **2010**, *16*, 1356–1364.

[25] C. Ci, J. J. Carbo, R. Neumann, C. de Graaf, J. M. Poblet, *ACS Catal.* **2016**, *6*, 6422–6428.

[26] N. Li, J. Liu, J. J. Liu, L. Z. Dong, S. L. Li, B. X. Dong, Y. H. Kan, Y. Q. Lan, *Angew. Chem. Int. Ed.* **2019**, *58*, 17260–17264; *Angew. Chem.* **2019**, *131*, 17420–17424.

[27] Q. Huang, J. Liu, L. Feng, Q. Wang, W. Guan, L.-Z. Dong, L. Zhang, L.-K. Yan, Y.-Q. Lan, H.-C. Zhou, *Natl Sci. Rev.* **2020**, *7*, 53–63.

[28] C. G. Morales-Guio, L.-A. Stern, X. Hu, *Chem. Soc. Rev.* **2014**, *43*, 6555–6569.

[29] J. A. Turner, *Science* **2004**, *305*, 972–974.

[30] B. Keita, U. Kortz, L. R. B. Holzle, S. Brown, L. Nadjo, *Langmuir* **2007**, *23*, 9531–9534.

[31] M. D. Symes, L. Cronin, *Nat. Chem.* **2013**, *5*, 403–409.

[32] B. Rausch, M. D. Symes, G. Chisholm, L. Cronin, *Science* **2014**, *345*, 1326–1330.

[33] R. Liu, G. Zhang, H. Cao, S. Zhang, Y. Xie, A. Haider, U. Kortz, B. Chen, N. S. Dalal, Y. Zhao, L. Zhi, C.-X. Wu, L.-K. Yan, Z. Su, B. Keita, *Energy Environ. Sci.* **2016**, *9*, 1012–1023.

[34] a) M. Arab Fashapoyeh, M. Mirzaei, H. Eshtiagh-Hosseini, A. Rajagopal, M. Lechner, R. Liu, C. Streb, *Chem. Commun.* **2018**, *54*, 10427–10430; b) A. A. Ensafi, E. Heydari-Soureshjani, B. Rezaei, *Int. J. Hydrogen Energy* **2017**, *42*, 5026–5034.

[35] a) G. Rousseau, L. M. Rodriguez-Albelo, W. Salomon, P. Mialane, J. Marrot, F. Doungmene, I.-M. Mbomekallé, P. de Oliveira, A. Dolbecq, *Cryst. Growth Des.* **2015**, *15*, 449–456; b) B. Nohra, H. El Moll, L. M. Rodriguez Albelo, P. Mialane, J. Marrot, C. Mellot-Draznieks, M. O'Keeffe, R. Ngo Biboum, J. Lemaire, B. Keita, L. Nadjo, A. Dolbecq, *J. Am. Chem. Soc.* **2011**, *133*, 13363–13374.

[36] N.-T. Suen, S.-F. Hung, Q. Quan, N. Zhang, Y.-J. Xu, H. M. Chen, *Chem. Soc. Rev.* **2017**, *46*, 337–365.

[37] Y. Zhang, J. Liu, S.-L. Li, Z.-M. Su, Y.-Q. Lan, *EnergyChem* **2019**, *1*, 100021.

[38] A. R. Howells, A. Sankarraj, C. Shannon, *J. Am. Chem. Soc.* **2004**, *126*, 12258–12259.

[39] S. Goberna-Ferrón, L. Vigara, J. Soriano-López, J. R. Galán-Mascarós, *Inorg. Chem.* **2012**, *51*, 11707–11715.

[40] J. Soriano-López, S. Goberna-Ferrón, L. Vigara, J. J. Carbó, J. M. Poblet, J. R. Galán-Mascarós, *Inorg. Chem.* **2013**, *52*, 4753–4755.

[41] F. M. Toma, A. Sartorel, M. Iurlo, M. Carraro, P. Parisse, C. Maccato, S. Rapino, B. R. Gonzalez, H. Amenitsch, T. Da Ros, L. Casalis, A. Goldoni, M. Marcaccio, G. Scorrano, G. Scoles, F. Paolucci, M. Prato, M. Bonchio, *Nat. Chem.* **2010**, *2*, 826–831.

[42] W. Luo, J. Hu, H. Diao, B. Schwarz, C. Streb, Y.-F. Song, *Angew. Chem. Int. Ed.* **2017**, *56*, 4941–4944; *Angew. Chem.* **2017**, *129*, 5023–5026.

[43] M. Blasco-Ahicart, J. Soriano-López, J. J. Carbó, J. M. Poblet, J. R. Galan-Mascaros, *Nat. Chem.* **2018**, *10*, 24–30.

[44] C. Costentin, S. Drouet, M. Robert, J.-M. Saveant, *Science* **2012**, *338*, 90–94.

[45] S. H. Szczepankiewicz, C. M. Ippolito, B. P. Santora, T. J. Van de Ven, G. A. Ippolito, L. Fronckowiak, F. Wiatrowski, T. Power, M. Kozik, *Inorg. Chem.* **1998**, *37*, 4344–4352.

[46] M. Girardi, S. Blanchard, S. Griveau, P. Simon, M. Fontecave, F. Bedioui, A. Proust, *Eur. J. Inorg. Chem.* **2015**, 3642–3648.